1230 *Chem. Mater.* **2001,** *13,* 1230−1237

Large Dynamic Ranges in Photorefractive NLO Polymers and NLO-Polymer-Dispersed Liquid Crystals Using a Bifunctional Chromophore as a Charge Transporter

David Van Steenwinckel,* Eric Hendrickx, and André Persoons

Laboratory for Chemical and Biological Dynamics, Center for Research on Molecular Electronics and Photonics, University of Leuven, Celestijnenlaan 200D, B-3001 Leuven, Belgium

Celest Samyn

Laboratory of Macromolecular and Physical Organic Chemistry, University of Leuven, Celestijnenlaan 200F, B-3001 Leuven, Belgium

Received August 8, 2000. Revised Manuscript Received January 23, 2001

We report on the synthesis and characterization of two photorefractive side-chain polymethacrylates, functionalized with amino-donor-containing chromophores. Carbazole units were neither copolymerized nor added to the polymers as separate components, and charge transport was provided by the chromophores. The polymer glass transition temperature was lowered to room temperature with appropriate plasticizers. After the addition of a sensitizer, (2,4,7-trinitro-9-fluorenylidene)malononitrile (TNFM) or C_{60}, a charge-transfer (CT) complex is formed between the chromophore and sensitizer, and photoconductivity can be observed upon excitation of the CT complex at 680 and 780 nm. The excellent photorefractive properties at both wavelengths were probed using the techniques of four-wave mixing and two-beam coupling. We show that the grating buildup speed is dominated by the charge generation. Because of the absence of carbazole units, the chromophore number densities in the samples are very high (up to 15.3×10^{20} cm^{-3}), leading to refractive index modulation amplitudes exceeding 5×10^{-3} at only 50 V/μm and 780 nm, which is among the best results obtained so far in polymeric photorefractive media. Meanwhile, the fully functionalized polymers offer the major advantage of a very good phase stability. As a proof of principle, we have also prepared polymer-dispersed liquid crystals (PDLC) using the bifunctional NLO polymers as the polymer matrix. PDLCs were prepared by a thermally induced phase separation after addition of 20 wt % of a liquid-crystal molecule that shows a nematic phase at room temperature. In the PDLC, a refractive index modulation amplitude of 1.8×10^{-2} was observed at 780 nm and 50 V/μm. To the best of our knowledge, this exceeds the refractive index modulation amplitudes observed so far in fully functionalized polymers at 780 nm.

Introduction

The photorefractive (PR) effect is based on a combination of photoconducting and electro-optic properties. Refractive index modulation amplitudes as high as 10^{-2} have been generated with a mW laser source.[1,2] Possible applications for PR materials are in the field of dynamic holography, such as optical correlation, phase conjugation, and optical image processing.[3] As a first strategy in organic photorefractive materials, the requirements for good photorefractive properties were provided by separate molecular components, each of which can be uniformly dissolved in a host polymer. Phase separation of the molecular dopants, however, leads to scattering and decreases the fringe contrasts. Replacing the photoconductive dopants in the inert polymer matrix by the photoconductive polymer poly(*N*-vinylcarbazole) (PVK) has been a major improvement. It has allowed the concentration of the charge transporter to be increased while crystallization of the carbazole groups was excluded.[4] In the PVK-based composite materials, the space-charge field is built up on a subsecond time scale because of the high photoconductivity provided by the PVK matrix. To achieve a high refractive index modulation amplitude, however, the photoconductive polymer also has to be doped with a large concentration of a strongly dipolar chromophore. Because chromophore

---

* To whom correspondence should be addressed.

[1] Kippelen, B.; Meerholz, K.; Peyghambarian, N. In *Nonlinear Optics of Organic Molecules and Polymers*; Nalwa, H. S., Miyata, S., Eds.; CRC: Boca Raton, FL, 1997; p 465.

[2] Moerner, W. E.; Grunnet-Jepsen, A.; Thompson, C. L. *Annu. Rev. Mater. Sci.* **1997**, *27*, 585.

[3] Günter, P.; Huignard, J.-P. In *Photorefractive Materials and Their Applications*; Springer: Berlin, 1988; Vols. 1 and 2.

[4] Sandalphon; Kippelen, B.; Peyghambarian, N.; Lyon, S. R.; Padias, A. B.; Hall, H. K. *Opt. Lett.* **1994**, *19*, 68.

10.1021/cm001159d CCC: $20.00

concentrations larger than 25 wt % are desirable, phase separation and crystallization of these chromophores from the apolar PVK matrix are a major problem. Efforts have been made to design chromophores with substituents that reduce the speed of phase separation.[5–7] Phase stability also has been improved using a eutectic chromophore mixture.[8] All this has resulted in guest–host systems with stability at room temperature for periods ranging from a few seconds to several years.

To completely eliminate chromophore crystallization, one could, through extensive synthesis, prepare fully functionalized PR polymers. For example, side-chain copolymers containing charge-transporting functionalities and chromophores have been prepared and have shown good PR performance.[9–11] In a previous paper, we described the synthesis and the photorefractive characteristics of a series of side-chain polymethacrylates.[12] The copolymers consisted of a polymethacrylate backbone with pendant carbazole and D-π-A-chromophore functionalities. Charge transport was provided mainly by the carbazole groups, while the D-π-A-chromophores were necessary to introduce electro-optic activity and birefringence. After reducing the glass transition temperature (T_g) of the polymers to the measurement temperature by plasticization, hence allowing for a periodically varying alignment of the anisotropic chromophores along the total electric space-charge field and the subsequent enhancement of the total refractive index modulation amplitude by birefingence,[13] the copolymers showed dynamic ranges that are comparable to those observed in the PVK-based composites. Therefore, the side-chain copolymers presented in ref 12 are a better alternative to photorefractive composites in applications where long-term stability is needed.

The dynamic range (i.e., the index modulation amplitude) of an organic PR polymer at a given electric field generally increases with increasing D-π-A-chromophore concentration, except for concentrations where electrostatic interactions between chromophores with large dipole moments start to attenuate the poling-induced acentric order.[14] With dipole moments smaller than 6 D, however, the latter effect only occurs at very large chromophore concentrations (2.0×10^{21} cm^{-3}). Therefore, to improve the PR performance, the highest possible chromophore concentrations are desirable. The upper limit for the chromophore concentration, if one wants to obtain thermally stable materials, is the critical concentration where crystallization can occur (generally below 5×10^{20} cm^{-3}, depending on the polarity and the T_g of the polymer matrix). In the previous work, the attachment of the chromophores to the polymer backbone allowed us to increase the total chromophore concentration up to 7.0×10^{20} cm^{-3} without noticeable crystallization.[12] Yet these fully functionalized polymers share an important shortcoming with the PVK-based composites. As the chromophore concentration is increased, the charge transport concentration is decreased dramatically, and the creation of the space-charge field through charge transport becomes more difficult. On the other hand, enlarging the charge transport concentrations results in decreasing chromophore concentrations and less electro-optic activity. This complicates the design of good materials because one has to find the optimal concentration ratio of charge-transporting functional groups to chromophores (NLO-functional groups).

One way to overcome this difficulty is to use a D-π-A-chromophore that can transport the charges by a hopping mechanism. To promote charge transport by migration of holes, a donor group with a small ionization potential is necessary. Several of these so-called bifunctional chromophores have been designed in the past and have been doped in an inert polymer matrix.[15,16] In this approach, again, crystallization of the dipolar chromophores is a major problem. Bifunctional chromophores have also been used to prepare organic glasses with improved phase stability.[17,18] These glasses, however, have some shortcomings as well. For instance, at low temperatures, organic glasses are very brittle and difficult to handle. Unlike polymers, glasses cannot be processed by extrusion techniques. In addition, glasses still are thermodynamically unstable, and crystallization will eventually occur. Attaching the bifunctional chromophores to a polymer backbone eliminates these shortcomings. Then, the high chromophore concentrations that can be achieved without crystallization not only are favorable for the Pockels effect and the orientational enhancement effect through birefringence but also facilitate the hopping of charges and hence the creation of a large space-charge field. The PR performance in such polymer systems is expected to increase dramatically with an increasing degree of functionalization. The scope of this work is to prove that high dynamic ranges can be obtained from functionalized polymers without carbazole moieties, where the pendant chromophore is the only charge-transporting medium. Compared to the previously developed multifunctional organic glasses, the functionalized polymers still have the advantages of a better processability, a larger tensile strength, and a larger resistivity against crystallization. In section II, we demonstrate, as a proof of principle, that using the NLO-functionalized polymers as a pho-

---

(5) Kippelen, B.; Marder, S. R.; Hendrickx, E.; Maldonado, J. L.; Guillemet, G.; Volodin, B. L.; Steele, D. D.; Enami, Y.; Sandalphon; Yao, Y. J.; Wang, J. F.; Röckel, H.; Erskine, L.; Peyghambarian, N. *Science* **1998**, *279*, 54.

(6) Hendrickx, E.; Wang, J. F.; Maldonado, J. L.; Volodin, B. L.; Sandalphon; Mash, E. A.; Persoons, A.; Kippelen, B.; Peyghambarian, N. *Macromolecules* **1998**, *31*, 734.

(7) Cox, A. M.; Blackburn, R. D.; West, D. P.; King, T. A.; Wade, F. A.; Leigh, D. A. *Appl. Phys. Lett.* **1996**, *68*, 2801.

(8) Meerholz, K.; Bittner, R.; De Nardin, Y.; Bräuchle, C.; Hendrickx, E.; Volodin, B. L.; Kippelen, B.; Peyghambarian, N. *Adv. Mater.* **1997**, *9*, 1043.

(9) Bolink, H. J.; Krasnikov, V. V.; Kouwer, P. H. J.; Hadziioannou, G. *Chem. Mater.* **1998**, *10*, 3951.

(10) Schloter, S.; Hofmann, U.; Hoechstetter, K.; Bäuml, G.; Haarer, D.; Ewert, K.; Eisenbach, C.-D. *J. Opt. Soc. Am. B* **1998**, *15*, 2560.

(11) Yu, L.; Chan, W. K.; Peng, Z.; Gharavi, A. *Acc. Chem. Res.* **1996**, *29*, 13.

(12) Van Steenwinckel, D.; Engels, C.; Gubbelmans, E.; Hendrickx, E.; Samyn, C.; Persoons, A. *Macromolecules* **2000**, *33*, 4074.

(13) Moerner, W. E.; Silence, S. M.; Hache, F.; Bjorklund, G. C. *J. Opt. Soc. Am. B* **1994**, *11*, 320.

(14) Harper, A. W.; Sun, S.; Dalton, L. R.; Garner, S. M.; Chen, A.; Kalluri, S.; Steier, W. H.; Robinson, B. H. *J. Opt. Soc. Am. B* **1998**, *15*, 329.

(15) Zhang, Y.; Ghosal, S.; Casstevens, M. K.; Burzynski, R. *Appl. Phys. Lett.* **1995**, *66*, 256.

(16) Silence, S. M.; Twieg, R. J.; Bjorklund, G. C.; Moerner, W. E. *Phys. Rev. Lett.* **1994**, *73*, 2047.

(17) Lundquist, P. M.; Wortmann, R.; Geletneky, C.; Twieg, R. J.; Jurich, M.; Lee, V. Y.; Moylan, C. R.; Burland, D. M. *Science* **1996**, *274*, 1182.

(18) Ogino, K.; Park, S.-H.; Sato, H. *Appl. Phys. Lett.* **1999**, *74*, 3936.

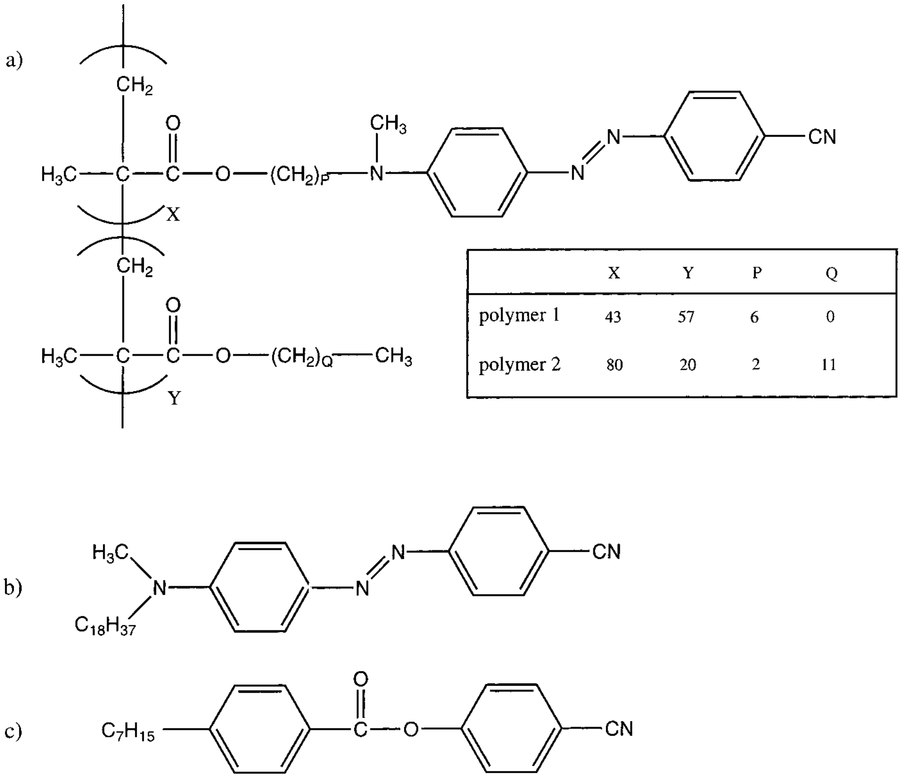

	X	Y	P	Q
polymer 1	43	57	6	0
polymer 2	80	20	2	11

Figure 1. (a) Structure of the functionalized polymethacrylates **1** and **2**. X and Y are mole fractions of the two building blocks, as determined by ^{1}H NMR and elemental analysis (see Supporting Information); P and Q are the spacer chain lengths. (b) Structure of chromophore **1**. (c) Structure of the liquid crystal (LC), discussed in section II.

Table 1. Composition of Samples 1–6

sample composition	copolymer **1** (wt %)	copolymer **2** (wt %)	DOP (wt %)	LC (wt %)	chromophore **1** (wt %)	TNFM (wt %)	C_{60} (wt %)	T_g (°C)[a]
1	70		10		19	1		22
2	70		10		19		1	23
3		69	10		20	1		31
4		79			20	1		46
5		70		19	10	1		26
6		60		19	20	1		12

[a] Glass transition temperature as determined by DSC, at a heating rate of 20 °C/min.

toconductive polymer matrix allows polymer-dispersed liquid crystals (PDLC) to be prepared. In these PDLCs, very high refractive index modulations (up to 1.8×10^{-2}) have been observed at 50 V/μm and 780 nm.

Results and Discussion

I. Photorefractive Properties of Side-Chain NLO Polymethacrylates. This section describes the photorefractive properties of the two fully functionalized NLO polymethacrylates, shown in Figure 1a. The synthesis and characterization details of the polymers are provided in the Supporting Information. The D-π-A-chromophore incorporated in the polymer shows an absorption maximum at 459 nm (ϵ = 39000 L mol^{-1} cm^{-1}) and a cutoff wavelength below 600 nm, enabling us to test all PR properties both at 780 and at 680 nm. In a previous study, we observed that chromophores with an amino donor group can have ionization potentials lower than carbazole.[19,20] When doped in PVK, these chromophores can act as a trapping site at low concentrations and can participate in the charge transport at high concentrations.[20,21] When doped in an inert polycarbonate matrix, photoconductivity is also observed. Thus, in a polymer system without carbazole, the chromophores are able to provide charge transport. Hence, a space-charge field can be formed by transporting the photogenerated charges created by excitation of the charge-transfer complex between the chromophore and an electron-deficient molecule, such as (2,4,7-trinitro-9-fluorenylidene)malononitrile (TNFM)[5] or C_{60}.

We have prepared six photorefractive samples (thickness: 125 μm) with compositions as listed in Table 1. Apart from large concentrations of charge transport agent and chromophores that can be obtained by a large degree of functionalization, photorefractive polymers should also have low glass transition temperatures (T_g) because the chromophores need sufficient free volume to reorient in the total electric field. Then, because of the large polarizability anisotropy of the chromophores, the refractive index modulation amplitude is strongly

---

(19) Van Steenwinckel, D.; Hendrickx, E.; Persoons, A.; Van den Broeck, K.; Samyn, C. *J. Chem. Phys.* **2000**, *112*, 11030.

(20) Hendrickx, E.; Van Steenwinckel, D.; Persoons, A.; Samyn, C.; Beljonne, D.; Brédas, J.-L. *J. Chem. Phys.* **2000**, *113*, 5439.

(21) Pai, D. M.; Yanus, J. F.; Stolka, M. *J. Phys. Chem.* **1984**, *88*, 4714.

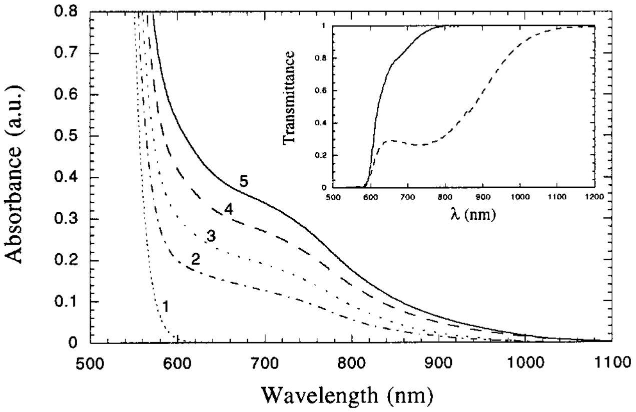

Figure 2. Curve 1: Absorption spectrum of 6 × 10^{-4} M of chromophore **1** in acetone. Curves 2−5: Absorption spectra of chromophore−TNFM in acetone. TNFM concentrations were 1.2 × 10^{-3}, 2.4 × 10^{-3}, 3.6 × 10^{-3}, and 4.8 × 10^{-3} M, respectively. The chromophore concentration was kept constant at 6 × 10^{-4} M in all solutions. Inset: Transmittance of sample **1**, sensitized with TNFM (dashed line), and sample **2**, sensitized with C_{60} (solid line). Both samples had a thickness of 125 μm.

enhanced by birefringence.[13] Copolymer **1**, which consists of functionalized and unfunctionalized methyl methacrylate units in a 43/57 molar ratio and has a T_g of 77 °C, is further plasticized in the PR sample preparation to allow for an efficient poling of the D-π-A-chromophores at ambient temperature. Because the refractive index modulation amplitude is directly proportional to the number density of the chromophores, as is predicted by the oriented gas model, it is efficient to use the chromophore as a plasticizer. Therefore, in the sample preparation, chromophore **1**, as shown in Figure 1b, is dispersed in the polymer matrix. Addition of chromophore **1** to polymer **1** lowers T_g and increases the chromophore concentration substantially. Care must be taken, however, that the guest chromophore concentration is kept below the critical concentration where phase separation occurs. The long alkyl chain incorporated in the chromophore provides an improved chromophore solubility and a very slow speed of phase separation. As a result, samples containing 20 wt % of chromophore plasticizer were stable for more than 3 months at 65 °C, even after a final adjustment of the sample T_g to room temperature, by addition of 10 wt % of an inert plasticizer (Dioctyl phthalate, DOP). Above 40 wt % concentration, crystallization occurs after only a few days at ambient temperature. To ensure long-term stability, all samples for photorefractive measurements in this work contain no more than 20 wt % of the dopant chromophore.

In a final step in the preparation of sample **1**, TNFM is added to the polymer mixture in 1 wt % concentration to provide photosensitivity at 680 and 780 nm. Similar to carbazole,[22] the chromophore forms a charge transfer complex with TNFM that is used to create the charges necessary to form the space-charge field. The complex shows maximum absorption at 725 nm and has useful absorption up to 1100 nm. In Figure 2, absorption spectra are shown from a series of solutions of chromophore **1** and TNFM in acetone. The chromophore concentration was kept constant at 6 × 10^{-4} M in all solutions. From curve 2 to curve 5, the TNFM concentration was increased by a factor of 4. Curve 1 shows the absorbance of a solution of chromophore **1** without TNFM. From this concentration series, we were able to determine the stability constant and the molar absorptivity of the complex formed between TNFM and the chromophore in solution, using the Benesi−Hildenbrandt equation.[23] Values of 19 M^{-1} and 1110 M^{-1} cm^{-1} were obtained, respectively.

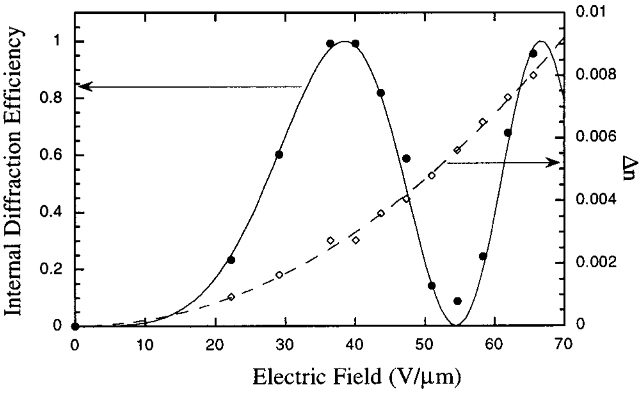

Figure 3. Internal diffraction efficiency and refractive index modulation amplitude versus applied electric field for sample **1** at 780 nm. The dashed line is a fit according to $\Delta n = a \cdot E^b$;[1] $a = 2.38 \times 10^{-6}$; $b = 1.94$. The solid line is a fit of the internal diffraction efficiency to $\eta = \sin^2(c \cdot \Delta n)$;[24] $c = 566$.

The diffraction efficiency of sample **1** at 780 nm as a function of the applied electric field was measured using a four-wave mixing setup (FWM) and is shown in Figure 3. Using Kogelnik's coupled wave theory for thick holograms, the amplitude of the refractive index modulation Δn can be calculated from the diffraction efficiency η using the following relationship.[24]

$$\eta = \sin^2\left(\frac{\pi d \Delta n}{\lambda(\cos \alpha_1 \cos \alpha_2)^{1/2}} \hat{e}_1 \cdot \hat{e}_2\right) \qquad (1)$$

In this equation d is the sample thickness, λ is the optical wavelength, α_1 and α_2 are the angles of the writing beams inside the sample with respect to the sample normal, and $\hat{e}_1$ and $\hat{e}_2$ are the polarization vectors of the incident reading beam and the diffracted beam, respectively. The index modulation amplitude in sample **1**, calculated from eq 1, is shown in Figure 3. Because of the high chromophore concentration and the low T_g (22 °C), the dynamic range of this material is among the highest reported so far in polymeric systems at a wavelength of 780 nm.[5,25,26] Hence, replacing the carbazole groups in more traditional carbazole-based composites by charge-transporting chromophores clearly is an important step toward more efficient materials because chromophore and charge transporter concentrations simultaneously can be very large.

The diffraction theory for thick gratings allows a calculation of the maximum refractive index modulation

---

(22) Gill, W. D. *J. Appl. Phys.* **1972**, *43*, 5033.

(23) Forster, R. In *Organic Charge-Transfer Complexes*; Academic Press: London, 1969.

(24) Kogelnik, H. *Bell. Syst. Techn. J.* **1969**, *48*, 2909.

(25) Würthner, F.; Wortmann, R.; Matschiner, R.; Lukaszuk, K.; Meerholz, K.; DeNardin, Y.; Bittner, R.; Bräuchle, C.; Sens, R. *Angew. Chem., Int. Ed. Engl.* **1997**, *36*, 2765.

(26) Schloter, S.; Hofmann, U.; Strohriegl, P.; Schmidt, H.-W.; Haarer, D. *J. Opt. Soc. Am. B* **1998**, *15*, 2473.

Table 2. Measured and Calculated Refractive Index Modulation Amplitudes and Chromophore Number Densities in Samples 1−6

sample	Δn_{780} at 50 V/μm[a]	$\Delta n_{780,\mathrm{max,th}}$ at 50 V/μm[b]	Δn_{680} at 50 V/μm[c]	N_c[d] (cm^{-3})
1	$(5.0 \pm 0.5) \times 10^{-3}$	$(5.4 \pm 0.5) \times 10^{-3}$	$(5.3 \pm 0.5) \times 10^{-3}$	10.9×10^{20}
2	$(4.6 \pm 0.5) \times 10^{-3}$	$(5.4 \pm 0.5) \times 10^{-3}$	$(6.0 \pm 0.5) \times 10^{-3}$	10.9×10^{20}
3	$(5.2 \pm 0.5) \times 10^{-3}$	$(6.9 \pm 0.5) \times 10^{-3}$		13.8×10^{20}
4	$(2.1 \pm 0.5) \times 10^{-3}$	$(7.6 \pm 0.5) \times 10^{-3}$		15.3×10^{20}
5	$(7.5 \pm 0.5) \times 10^{-3}$	$(7.3 \pm 0.5) \times 10^{-3}$	$(8.2 \pm 0.5) \times 10^{-3}$	12.5×10^{20}
6	$(18.0 \pm 0.5) \times 10^{-3}$	$(7.6 \pm 0.5) \times 10^{-3}$		13.2×10^{20}

[a] The refractive index modulation calculated from the experimental diffraction efficiencies at 780 nm and 50 V/μm via eq 1. [b] Value of the refractive index modulation amplitude that can theoretically be obtained at 780 nm and 50 V/μm from the diffraction theory for thick gratings.[1] For samples **5** and **6**, the contributions from the LC were taken into account, assuming uncorrelated molecules (no cooperative alignment). [c] The refractive index modulation calculated from the experimental diffraction efficiencies at 680 nm and 50 V/μm via eq 1. [d] The chromophore number density, calculated using a polymer density of 1.1 g cm^{-3}.

Table 3. Grating Buildup Times, Photoconductivities, and Absorption Coefficients of Samples 1 and 2 at 680 and 780 nm

	τ_{680} (s)[a]	τ_{780} (s)[b]	$\sigma_{\mathrm{ph},680}$ (pS/cm)[c]	$\sigma_{\mathrm{ph},780}$ (pS/cm)[d]	α_{680} (cm^{-1})[e]	α_{780} (cm^{-1})[f]
sample **1**	28 ± 4 ($\beta = 0.78$)	60 ± 8 ($\beta = 0.77$)	0.38 ± 0.05	0.23 ± 0.05	44 ± 0.5	42 ± 0.5
sample **2**	19 ± 4 ($\beta = 0.82$)	218 ± 30 ($\beta = 0.83$)	0.50 ± 0.05	0.06 ± 0.05	8 ± 0.5	<0.5

[a] Grating buildup time measured in a FWM setup at 680 nm, an applied field of 32 V/μm, and writing intensities of 3 W/cm^2, using a stretched exponential fit (Supporting Information). [b] Grating buildup time measured in a FWM setup at 780 nm, an applied field of 32 V/μm, and writing intensities of 3 W/cm^2, using a stretched exponential fit (Supporting Information). [c] Photoconductivity measured at 680 nm, an intensity of 0.1 W/cm^2, and an applied field of 64 V/μm. [d] Photoconductivity measured at 780 nm, an intensity of 0.1 W/cm^2, and an applied field of 64 V/μm. [e] Absorption coefficient at 680 nm. [f] Absorption coefficient at 780 nm.

amplitude, $\Delta n_{\mathrm{max,th}}$, that can theoretically be achieved (see Supporting Information).[1] In these expressions, the linear polarizability anisotropy, the dipole moment, the first hyperpolarizability, and the chromophore number density are taken into account. In Table 2, $\Delta n_{\mathrm{max,th}}$ for sample **1**, calculated for an external field of 50 V/μm and at 780 nm, is shown, along with the experimental Δn at that field strength. The measured index modulation amplitude is slightly smaller than the maximum value that can be achieved according to the oriented gas model. Possibly, this stems from the fact that in the calculations we have assumed that the space-charge field is saturated. Because of a low photogeneration efficiency (discussed below), however, the space-charge field probably is not completely saturated. For sample **1**, we have also measured the refractive index modulation amplitude of a grating written at a wavelength of 680 nm (also shown in Table 2) in the same four-wave mixing setup. Compared to the results obtained at 780 nm, the index modulation amplitude was increased by a factor of 1.06 because of a small wavelength dispersion of $\Delta\alpha$.[27] The $\Delta n_{\mathrm{max,th}}$ at 680 nm amounts to 6.3×10^{-3}.

To verify that the polymers are photorefractive, we have proven the nonlocal, photorefractive nature of the grating by asymmetric two-beam coupling.[3] In this experiment, we have observed that the direction of energy transfer changed upon reversal of the direction of the applied electric field. At a field of 65 V/μm, the two-beam coupling gain coefficient for sample **1** exceeded 100 cm^{-1}. It is important to note that all measurements were performed in the thick grating regime.

We have investigated the grating buildup dynamics at 680 and 780 nm. The grating buildup times were determined in FWM experiments by fitting the curves of the diffraction efficiency versus time using a stretched exponential function (see Supporting Information). The buildup times of sample **1** at 680 and 780 nm are shown in Table 3, along with the photoconductivities and the absorption coefficients at both wavelengths. A good correlation is observed between the photoconductivities and the PR grating buildup rates at both wavelengths. Compared to the measurements at 780 nm, the grating buildup speed at 680 nm in sample **1** was increased by a factor of 2.1, while also a larger photoconductivity was measured at 680 nm (see Table 3).

The grating buildup rate of a PR grating can be determined by the photogeneration efficiency of the charges, by the migration and trapping dynamics of these charges,[28] or by the rotational mobility of the chromophores. The measurements of the buildup rates at two different wavelengths allow us to determine which step in the grating formation is rate-limiting. In the PR grating formation, charge generation is dependent on the wavelength, while migration of the charges and rotational flexibility of the chromophores are not. The grating formation speed and the photoconductivity being dependent upon the excitation wavelength hence indicate that charge generation is the rate-limiting factor rather than the charge mobility or the time needed for chromophore reorientation. Moreover, because the used intensities and the absorption coefficients at 680 and 780 nm are comparable and hence equal amounts of energy are absorbed, it can be concluded that the photogeneration efficiency of the CT complex is higher at 680 nm than at 780 nm. As was expected, sample **1** shows a slow grating buildup at both wavelengths because of the large energetic disorder in a system containing a high concentration of strongly dipolar molecules and a correspondingly low charge mobility[29] and photogeneration efficiency.[30] This is also evidenced by the very small photoconductivity in the sample, which is a convolution of the charge mobility and the photogeneration efficiency.

---

(27) Sandalphon; Wang, J. F.; Kippelen, B.; Peyghambarian, N. *Appl. Phys. Lett.* **1997**, *71*, 873.

(28) Hofmann, U.; Grasruck, M.; Leopold, A.; Schreiber, A.; Schloter, S.; Hohle, C.; Strohriegl, P.; Haarer, D.; Zilker, S. J. *J. Phys. Chem.* **2000**, *104*, 3887.

(29) Bässler, H. *Phys. Stat. Sol. (b)* **1993**, *175*, 15.

(30) Hendrickx, E.; Kippelen, B.; Thayumanavan, S.; Marder, S. R.; Persoons, A.; Peyghambarian, N. *J. Chem. Phys.* **2000**, *112*, 9557.

The composition of sample **2** is very similar to that of sample **1** except that the sensitizer TNFM has been replaced by C_{60} (see Table 1). The buildup times and the photoconductivities of this sample, together with the absorption coefficients of the samples, are listed in Table 3. At 780 nm, sensitizing polymer **1** with C_{60} instead of TNFM led to a much slower grating buildup and a small decrease of the dynamic range. As shown in Table 3 and the inset of Figure 2, which shows the transmittance of samples **1** and **2** versus wavelength, the chromophore−C_{60} complex has only very small absorption at 780 nm. This explains the slow grating formation and suggests that the space-charge field would be less saturated, leading to a smaller measured Δn (see Table 2) at 780 nm. At 680 nm, however, sample **2** shows an absorption coefficient of 8 cm^{-1}. Consequently, more charges are generated per time unit, and the grating buildup is substantially faster. At 680 nm, the grating buildup rate is even significantly larger than that in sample **1**, although the absorption coefficient, and hence the amount of absorbed photons per second, of the latter sample is 5.5 times higher. This is explained by the larger photogeneration quantum efficiency from the C_{60}−chromophore complex at that wavelength, compared to the TNFM−chromophore complex. Consequently, as is suggested by the larger measured Δn at 680 nm, the space-charge field gets closer to saturation. The faster grating buildup at 680 nm upon replacing TNFM with C_{60} as the sensitizer again indicates that charge generation is the rate-limiting step, as was anticipated above. Again, a good correlation is found between the photoconductivities and the grating buildup rates.

In an attempt to obtain higher dynamic ranges through larger chromophore concentrations, a copolymer with 80 mol % pendant chromophore units with ethyl spacer and 20 mol % methyl methacrylate units was prepared in a second polymerization. The T_g of the resulting polymer, however, was too high (130 °C) to enable efficient poling of the chromophores. Therefore, in a third copolymerization, the 20 mol % methyl methacrylate was replaced by dodecyl methacrylate to obtain polymer **2**. The long dodecyl chain provides additional free volume and reduces the T_g of the resulting polymer to 98 °C. A sample containing polymer **2**/chromophore **1**/DOP/TNFM in a 69/20/10/1 ratio (sample **3**, $T_g = 31$ °C) was prepared. The observed Δn at 50 V/μm is listed in Table 2, along with the maximum obtainable $\Delta n_{\max,\mathrm{th}}$. The difference $\Delta n_{\max,\mathrm{th}} - \Delta n$ being larger for sample **3** than for the samples **1**−**2** indicates that T_g for this sample is too high. Indeed, when the experimental temperature for this sample is increased (up to 32 °C), higher Δn values (up to 6.0×10^{-3}) were obtained in sample **3**. Such a large increase of Δn with temperature was not observed in samples **1** and **2** and indicates that the chromophores in the latter samples have sufficient free volume at room temperature to enable reorientation on a time scale of tens of seconds. Increasing the chromophore density of sample **3** by substituting 10 wt % of DOP by 10 wt % of polymer **2** (sample **4**, $T_g = 46$ °C) reduced Δn to 2.1×10^{-3} at 50 V/μm and 21 °C, again because of a higher T_g for this mixture.

It is clear that copolymers **1** and **2** both show excellent PR properties. In copolymer **2**, the fraction of chromophore-functionalized units was increased in an attempt to improve the dynamic range. From the above measurements on polymer **2**, however, it is clear that the factor limiting the dynamic range at this stage is the high T_g of the copolymers and not the chromophore concentration. A further increase in the degree of functionalization up to 100% led to polymers with low solubility, hampering the device preparation, and even higher T_g values (150 °C), preventing the orientational enhancement effect to take place. One way to overcome this problem is to add efficient inert plasticizers. Unfortunately, the net chromophore concentration then is again reduced. Adding more chromophore as plasticizer (above 30 wt %) reduces the phase stability. Hence, the solution to this problem would be provided by polymers with lower T_g or by the addition of a plasticizer that also affects the refractive index modulation in a positive way. The synthesis of polymers having a lower T_g should be a major topic in further research. How the dynamic range can be further improved by adding a liquid-crystal dopant is discussed in section II.

II. Preparation of PDLCs Using Polymer 2. In section I we discussed the photorefractive performance of two polymethacrylates plasticized with dioctyl phthalate (DOP). Here, we provide a proof of principle that the synthesized polymers can be used in the preparation of efficient polymer-dispersed liquid crystals (PDLCs).[31,32] In a PR PDLC, charge generation and transport take place through the polymer matrix, whereas the change in liquid-crystal droplet configuration and orientation provides the index modulation. In contrast to chromophores dispersed in polymers, liquid-crystal (LC) molecules in the mesophase can be oriented at much lower electric fields. In pure LC, however, the PR performance is poor for small fringe spacings (<5 μm) because of the large domain size and the resulting low resolution. PDLCs combine the advantages of LC and polymers, allowing for low field reorientation of the LC in the mesophase and high resolution (small droplets), hence increasing the dynamic range of the materials.[32] This results in refractive index modulations that can be larger than the value that is predicted from the diffraction theory ($\Delta n_{\max,\mathrm{th}}$), assuming uncorrelated molecules. In the PR PDLCs prepared thus far, the polymer matrix did not contribute to the index modulation amplitude. By using bifunctional copolymer **2** as the PDLC matrix, the matrix will provide charge transport but will also contribute to the index modulation amplitude. As functionalized polymers allow for large charge-transporter and chromophore concentrations, outstanding photorefractive properties are expected from these materials.

Generally, PDLCs are prepared by a thermally induced phase separation of the liquid crystal (LC) from the polymer matrix by rapid cooling, after heating the mixture above the melting temperature of the polymer binder. LC droplets form as the polymer starts to harden, and the droplets grow until the glass transition region of the polymer is crossed. PR PDLCs with 30 wt

---

[31] Ono, H.; Kawatsuki, N. *Opt. Lett.* **1997**, *22*, 1144.

[32] Golemme, A.; Volodin, B. L.; Kippelen, B.; Peyghambarian, N. *Opt. Lett.* **1997**, *22*, 1226.

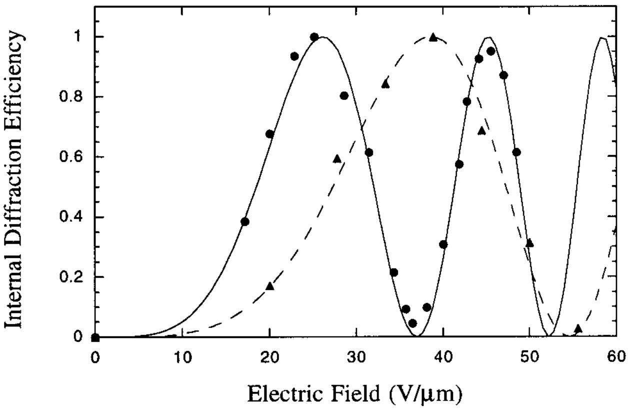

Figure 4. Internal diffraction efficiencies of samples **5** (triangles) and **6** (circles) versus electric field. Fits are according to $\eta = \sin^2(c\cdot\Delta n)$;[24] triangles, $c = 565$; circles, $c = 566$.

% of LC have been prepared.[31,32] These samples were opaque but turned to a transparent state upon application of an electric field because of a reorientation of the LC director. Samples **5** and **6** (composition, see Table 1) were prepared by a thermally induced phase separation. The polymer–LC mixture (containing only 19 wt % of LC) was homogenized mechanically at a temperature of 110 °C, which is above the melting temperature of the polymer. After the sample assembly, the sample was quench-cooled to room temperature. At this point, although not completely opaque, sample **5** ($T_g = 26$ °C) showed the transmission characteristics of a PDLC, with an 18% transmittance increase upon application of a bias field of 40 V/μm. This transmittance change was fully reversible. In sample **6**, compared to sample **5**, 10 wt % of polymer **2** was replaced by 10 wt % of chromophore **1**, resulting in a lower T_g (12 °C). This lower T_g allows for a better phase separation of the LC and polymer and hence more pronounced PDLC characteristics. In sample **6**, an 80% increase in transmittance is observed upon application of a field of 40 V/μm. In this sample, small droplets were observed under an optical microscope. When placed between two crossed polarizers, light was transmitted through the droplets, indicating birefringence and hence also crystallinity in those domains. Combined with the observation that samples without LC did not show the phase-separated domains, it leads to the conclusion that the small domains must contain LC in the mesophase, evidencing that we have obtained PDLCs. When 10 wt % of LC from sample **6** is replaced by 10 wt % of polymer **2**, no birefringence is observed between two crossed polarizers, nor does the sample show an increased transmittance upon application of an electric field. Clearly, at the remaining 10 wt % LC concentration, the critical concentration necessary for phase separation is not achieved. Also, the samples from section I, containing DOP instead of LC, did not show birefringence, phase separation, or an increased transmittance upon field application.

The diffraction efficiency of sample **5** is shown in Figure 4 (dashed line). The first maximum in diffraction efficiency already occurs at 38 V/μm, while a second maximum (not shown) was observed at 66 V/μm. The maximum diffraction efficiency at the second peak was smaller than that at the first peak because a small fraction of the energy is coupled into higher diffraction orders, although s-polarized writing beams are used, and coupling is reduced to a minimum. The diffraction efficiency of sample **6** ($T_g = 12$ °C) is also shown in Figure 4 (solid line). The first maximum in diffraction efficiency occurs at 25 V/μm, and the second peak is found at 45 V/μm. This unshown performance is a very good proof of principle that outstanding dynamic ranges can be obtained in NLO-polymer-dispersed liquid crystals with a bifunctional chromophore.

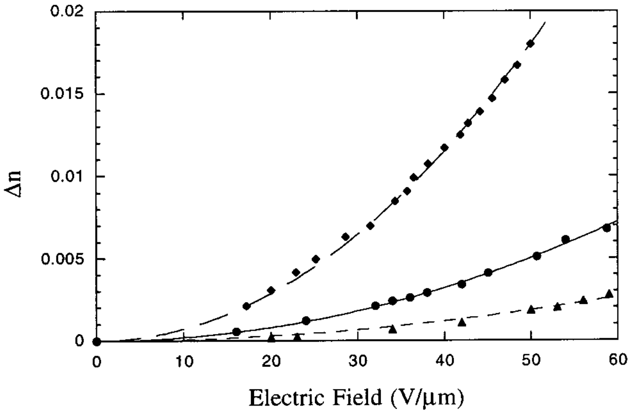

Figure 5. Refractive index modulation amplitude at 780 nm as a function of applied electric field for a PR sample with (sample **6**, diamonds) and without (sample **3**, circles) liquid crystal. Triangles are for a reference sample composed of DMNPAA:PVK:ECZ:TNF in a 50:33:16:1 wt ratio, measured at 675 nm.[33] Fits according to $\Delta n = b\cdot E^c$;[1] diamonds, $b = 1.0 \times 10^{-5}$, $c = 1.91$; circles, $b = 2.4 \times 10^{-6}$, $c = 1.95$; triangles, $b = 8.7 \times 10^{-7}$, $c = 1.96$.

Similar to the samples from section I, we have listed calculated Δn values of samples **5** and **6** in Table 2. Having a larger chromophore density and a lower T_g, the dynamic range of sample **6** is much larger than that of sample **5**. From Table 2, it is clear that the maximum value that can theoretically be obtained, $\Delta n_{\mathrm{max,th}}$, calculated from the PR Figure-of-Merit and the chromophore and liquid-crystal number densities, is largely exceeded in sample **6**. In this theoretical value, the additional contribution of the liquid crystal's PR Figure-of-Merit to the refractive index modulation through birefringence was accounted for, assuming uncorrelated molecules. In sample **5**, the measured Δn at 50 V/μm is also slightly higher than the theoretical maximum value that can be achieved, while for all samples without LC (samples **1**–**4**) the Δn values are clearly below this maximum value, probably because of a nonsaturated space-charge field. Because no charge-transfer complex could be observed between the liquid crystal and TNFM or the chromophore, however, there is no reason to believe that the space-charge field in samples **5** or **6** would be closer to saturation than in the previous samples. This indicates that, in both samples, the formation of a PDLC, where the assumption of uncorrelated molecules is no longer valid and where the refractive index grating is enhanced by the cooperative reorientation of the liquid-crystal molecules in the spatially modulated space-charge field, would be responsible for the enhancement of the PR effect.

Figure 5 quantitatively illustrates the efficiency of doping the polymers with 20 wt % of LC. It shows the Δn of samples **3** and **6** versus electric field. As a reference, we have added the Δn of a PVK composite containing 50 wt % of the azo dye 2,5-dimethyl-4-(*p*-nitrophenylazo)anisole (DMNPAA), as a function of electric field, measured at 675 nm.[33] Without LC, the newly synthesized polymethacrylates already are more efficient than the DMNPAA composite. When 20 wt % LC is added, a supplementary increase in Δn by a factor of 3.6 is observed, although the chromophore densities in samples **3** and **6** as well as the $\Delta n_{\mathrm{max,th}}$, assuming uncorrelated molecules, are almost equal.

Note that because the T_g of the binder polymer is around room temperature, the phase separation of the LC in samples **5** and **6** continued gradually, giving rise to larger LC domains and loss of transparency. In sample **6**, because of the lower T_g, the whole process of phase separation was much faster compared to that of sample **5**. Sample **5** turned completely opaque on a time scale of 2 months, whereas for sample **6** this process took only 2 weeks at ambient temperature. The much faster phase separation would also explain the large difference between the dynamic range of samples **5** and **6**. In sample **6**, the low T_g allows for a better reorientation of the chromophores and a larger contribution of birefringence to the refractive index modulation, and also it improves the possible pathways for a phase separation and redistribution of the LC molecules. Hence, a larger portion of LC undergoes phase separation, and more pronounced PDLC characteristics can be observed. The larger diffraction efficiencies in sample **6**, compared to those in sample **5**, combined with the faster phase separation again indicate that the enhancement of the PR effect is controlled by the phase separation of the LC from the polymer and the formation of a PDLC.

Conclusion

In summary, we have observed outstanding photorefractive properties in methacrylic copolymers functionalized with pendant dipolar chromophores, doped with small amounts of chromophore, inert plasticizer, and a sensitizer. The polymers do not contain a carbazole group, and the chromophore acts as the charge-transporting species. The benefit of having only one moiety that transports the charges and produces the electro-optic effect at the same time is that high concentrations can be used to obtain a large dynamic range. We were able to determine that the large response times for the mixtures are due to low charge generation efficiencies. We have demonstrated, as a proof of principle, that the synthesized methacrylic copolymers can also be used in the preparation of PDLCs. In the PDLCs, the refractive index modulations are enhanced by a factor of 3.6. Index modulations of 1.8×10^{-2} were obtained at a field of 50 V/μm and at 780 nm. To the best of our knowledge, this is the first time that NLO polymers are used in the preparation of PDLCs and that two diffraction maxima can be observed in an organic medium below an externally applied field of 45 V/μm. A drawback of the material is that, as was discussed above, the LC droplets continue to grow slowly. This explains why the PR properties of the samples decrease after a few weeks (loss of resolution as the LC domains become bigger) and why the samples turn opaque eventually. A possible solution to this problem would be provided by a system where T_g is kept slightly above room temperature, hence preventing the droplets to enlarge, but maintaining the good PR properties. In addition, the droplet size in PDLCs is affected by the cooling rate of the polymer melt/LC solution during the sample preparation. Fast cooling rates tend to produce small droplets because there is not sufficient time for large particles to form. The size of the droplets will influence the resolution of the technique, but probably also the charge transport in the mixture and the magnitude of the effects. Therefore, more extensive studies for the optimization of these materials are necessary.

Acknowledgment. D.V.S. is a research assistant and E.H. is a research associate of the Fund for Scientific Research-Flanders (Belgium) (FWO). The authors thank K. Binnemans and C. Engels for the characterization of the liquid crystal. This research was supported by research grants from the FWO (G.0338.98 and S 2/5−AV. E 8), the University of Leuven (GOA/2000/03), and the Belgian Government (IUAP P4/11).

Supporting Information Available: Synthesis schemes and characterization data of the liquid crystal and the two copolymers (250 MHz ^{1}H NMR, elemental analysis, GPC, DSC measurements). Photorefractive sample preparation and characterization (four-wave mixing, two-beam coupling, buildup dynamics, and photoconductivity measurements). Discussion of how the values of $\Delta n_{\mathrm{max,th}}$ in Table 2 were obtained (PDF). This material is available free of charge via the Internet at http://pubs.acs.org.

CM001159D

---

[33] Volodin, B. L.; Sandalphon; Meerholz, K.; Kippelen, B.; Kukhtarev, N. V.; Peyghambarian, N. *Opt. Eng.* **1995**, *34*, 2213.